In: 2023 IEEE/AIAA 42nd Digital Avionics Systems Conference (DASC), 1-5 October 2023, Barcelona, Spain
DOI:10.1109/DASC58513.2023.10311149

A Risk-Based UAM Airspace Capacity Assessment Method Using Monte Carlo Simulation

Yu Su, Yan Xu, Gokhan Inalhan
School of Aerospace, Transport and Manufacturing
Cranfield University
Bedford, United Kingdom
(yu.su, yanxu, inalhan)@cranfield.ac.uk

***Abstract*—Inspired by risk analysis assistance service and dynamic capacity management service in U-space service, this paper investigates a risk-based UAM airspace capacity assessment method using Monte Carlo simulation for future urban air mobility. The quantitative risk assessment of the flight plan is divided into three parts: the ground / air risks of the flight plan and the mid-air collision risk between UAM. Using the comprehensive risk assessment method, this paper generates several simulation scenarios in the airspace to be evaluated in terms of the type of participants, the presence of the detect and avoid system, and the total number of participants in the airspace, conducts Monte Carlo simulations, and records the simulation data for analysis. Through the analysis of simulation data, it is found that the maximum risk of UAM in airspace increases with the increase of the number of airspace invaders and the total number of UAM. However, the maximum risk of UAM in airspace decreases when the aircraft in airspace contains the detection and avoid system with the same other conditions. Based on simulation data, this paper informatively proposes the concept of a 3D risk surface and a risk-based airspace capacity envelope, using the horizontal surface formed by a specific risk threshold to cut the 3D risk surface to form an airspace capacity envelope, which visually describes the number of aircraft that can be contained in the airspace under a specific risk threshold.**

***Index Terms*—urban air mobility, capacity assessment, Monte Carlo simulation**

I. Introduction

A. Research background

In the urban aerial environment, the unmanned aircraft system (UAS) and small manned aircraft are already being applied for various purposes such as traffic monitoring [1] nowadays. In addition, they are plans for smart cities in the near future [2], [3] and a core component of Urban Air Mobility (UAM) [4].

UAM enables cooperative, highly automated, cargo delivery or passenger air transportation services in and around urban areas. In the popularization of UAM, integrating UAM into urban and suburban airspace is challenging, as it entails risks from a safety perspective. For the low-altitude urban airspace of the future, there is an urgent need to address the issue of how to engage more UAM and operate efficiently while ensuring mission safety. For complex urban airspace with a mix of manned aircraft and UAVs, they are currently only subject to conservative and uniform flight restrictions. Such restrictions can severely constrain UAM operations, especially in densely populated areas. A more adaptive and intelligent approach is needed to identify the maximum number of aircraft that can be deployed in airspace within an acceptable level of risk.

B. Previous work

Europe has developed a vision called U-Space to facilitate the phased introduction of procedures and a set of services for safe, efficient, and secure access to airspace for large numbers of drones. In the blueprint of U-space services, risk analysis assistance and flight plan preparation / optimization are both identified as extended U2 services in CORUS. Fig. 1 shows the frame diagram of U-space services. The two red squares in it represent risk analysis assistance service and dynamic capacity management service respectively.

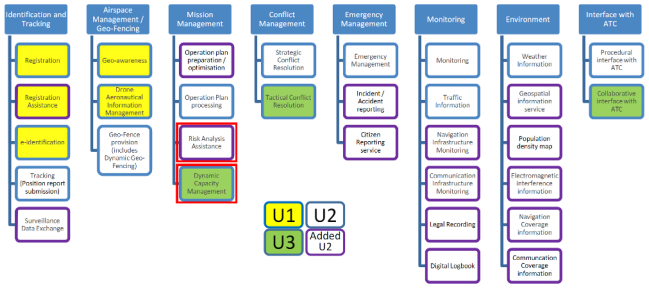

Fig. 1. U-space services, the two services marked in red are the services that can be implemented by the method proposed in this paper [5].

The service called risk analysis assistance will perform risk assessment to the preliminary flight plan [6]. For risk assessment, Joint Authorities for Rulemaking on Unmanned Systems (JARUS) has developed the Specific Operational Risk Assessment (SORA). It is a novel approach which can evaluate the risk level of an UAS operation plan [7]. For the risk assessment to the preliminary flight plan, SORA focuses on assigning to an UAS operation two classes of risk, a ground risk class (GRC) and an air risk class (ARC). The SORA allows operators to utilise certain or mitigating measures to reduce both risk-classes [8], [9]. Ref [10]–[12] proposes the concept of risk cost map that associates discretized locations of the space with a suitable risk cost and the generation of guided flight plans with the risk cost map. In addition to SORA,

Ref [13] proposes risk assessment models of UAS over road networks. Going further, they investigated the feasibility of a long-range railway inspection mission by UAS [14].

The service called dynamic capacity management aims to match demand with capacity and has two threads. Demand may be regulated to match capacity, or capacity may be changed to match demand. In this service, there is first a process to predict the number of aircraft that can be accommodated in a given airspace and, once the airspace capacity is obtained, to determine whether the airspace is full. If the airspace is full, solutions include suggesting delayed flights or suggesting that some aircraft be diverted out of the full airspace [15]. The current approach to civil aviation airspace balancing demand and capacity is to divide the airspace into sectors. Each sector has a capacity threshold in the form of a maximum number of aircraft for a given time period. This threshold is used as a controller workload limit indicator for each sector, regardless of traffic complexity [16]. As the first stage of the service, research on airspace capacity estimation dates back to decades ago [17] research of airport runway capacity. Subsequently, the capacity estimation theories for airports [18], regional [19], and terminal areas [20]–[22] capacity estimation theories have been proposed accordingly.

C. Research gap

For the risk assessment of UAM flight plans, many risk assessment models are currently targeted at specific objects. For example, Ref [13] and [14] put forward the risk assessment of the ground roads for the flight plan; Ref [23]–[26] focus on the risks of ground areas or buildings; Ref [27] focuses on risks in airspace. However, in the actual UAM operation process, there will be air and ground risks, which requires a risk assessment model to comprehensively assess mission risks. SORA process is also far from complete. The GRC/ARC lookup table is based on a simple scoring. Finally, after the risk assessment of the flight plan, how to optimize it is a problem to solve.

For the assessment of UAM airspace capacity, most research has focused on civil aircraft and the airport and its surroundings [18]–[22]. But for the future urban low altitude airspace, both in terms of the flight performance of air traffic participants and the mission airspace characteristics of urban low altitude area are very different from the traditional civil aviation aircraft and airport environment. Considering the future mixed mission scenario of manned and unmanned aircraft for urban air traffic, some scholars have conducted research on the assessment of UAV capacity in low-altitude airspace. Ref [28], [29] use a mathematical definition based on thresholds to estimate the capacity of UAV traffic in low-altitude uncontrolled airspace based on safety and performance considerations. But conflict is simply defined as a loss of minimum separation. However, in actual urban mission flying, it is also clear that a variety of potential threats cannot be ignored, rather than focusing solely on the loss of minimal separation. Future UAM system operations will tend to be free-flying in nature, i.e. individual aircraft will be responsible for determining their own routes. The U-space service provider (USSP) should therefore support user-preferred flight paths wherever possible [30]. A number of 'self-separation' design concepts and decentralised control strategies that transfer responsibility for these separations to the aircraft have been proposed to increase the capacity of aircraft [31], [32]. However, the theoretical methods used to measure such airspace capacity are not well elaborated.

II. Motivation

Inspired by the risk analysis assistance service and dynamic capacity management service, the research motivation of this paper is to combine them to achieve UAM mission airspace capacity assessment and management. Monte Carlo simulation is used to randomly generate mission scenarios in airspace and set risk thresholds to assess the risk of each mission scenario. A comprehensive risk assessment for air and ground properties is performed for each scenario, including UAM with known flight plans and intruders with unknown flight plans. The safety capacity of the airspace is analyzed by counting the number of scenarios that exceed a set risk threshold under different constraints. The assessed risk-based maximum capacity of the mission airspace provides an important "capacity" reference for demand and capacity balancing (DCB) in future UAM applications. The flow chart of this method is shown in Fig. 2.

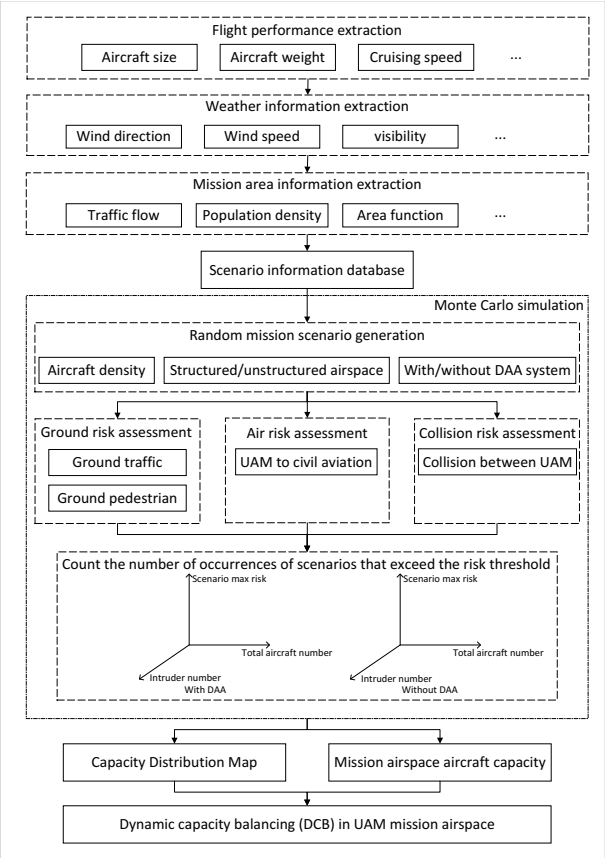

Fig. 2. Flow chart of the proposed risk-based UAM mission airspace capacity assessment method.

In this paper, as shown in Fig. 2, the entire UAM airspace capacity assessment methodology is divided into three main components: mission airspace aircraft and environmental information extraction, mission airspace aircraft risk assessment, and sampling-based mission airspace capacity estimation.

For the information extraction step, both static and dynamic information related to the mission will be extracted. Static information includes aircraft performance parameters. Dynamic information includes historical weather information, historical population density information and traffic in the mission area. This information will be stored in the mission scenario information database for use in subsequent Monte Carlo simulations.

For the risk assessment step, multiple representative mission scenarios will be generated using the program. The generation of scenarios considers the impact of different constraints and some combination of probability distributions. Constraints include the density of aircraft in the airspace, the proportion of structured traffic (aircraft with flight plans) in the airspace, and whether the aircraft in the airspace includes a Detect and Avoid (DAA) system. The probability includes the aircraft's own failure rate, air collision rate, etc. Environmental information will be extracted from the scenario information database to generate simulation scenarios. Generated scenarios will be assessed for comprehensive risk.

Finally, the number of mission scenarios that exceed the risk threshold in the simulation is counted according to the risk threshold, and the probability of occurrence of high-risk scenarios under different constraints is then analysed. Based on the probability of occurrence of high-risk scenarios at different aircraft densities under a given condition, the safe aircraft capacity of the airspace under that condition can be estimated.

In the field of airspace capacity assessment, this research innovatively proposes a risk based UAM mission airspace capacity assessment method. This research uses a mathematical definition based on risk thresholds to analyze and estimate UAM traffic capacity in urban or suburban low-altitude airspace from the perspective of air and ground property safety using sampled data from Monte Carlo simulations. The airspace security capacity assessed by the research will provide an important capacity reference for the DCM service.

III. Mission scenario risk assessment

As mentioned above, this research will combine two services, risk analysis assistance and dynamic capacity management, to perform a risk-based airspace capacity assessment of mission UAM in urban airspace. The idea of the research is to estimate the safe aircraft capacity of the airspace with different input parameters by using Monte Carlo simulations. The parameters such as maximum risk and number of simulations exceeding the defined risk threshold of the airspace for different airspace aircraft densities, airspace structures and flight route types will be obtained. In this section, the risk assessment model for mission scenarios is described.

A. Flight performance extraction

In order to assess the specific value of the risk cost of a flight plan, it is necessary to estimate the probability of an aircraft's accident and the severity of the damage caused. The probability of an accident is related to the type and size of the aircraft, and the severity of the accident is related to the quality of the aircraft and its flight performance.

In this paper, we consider two types of aircraft with different flight characteristics, namely fixed-wing aircraft and rotorcraft. For the dimensional data of the aircraft, consider the length l and width w of the aircraft, wing area S, as well as the horizontal windward area $A_{horizontal}$ and the vertical projection area $A_{vertical}$.

In addition to the vehicle size parameters, it is also necessary to obtain the performance parameters of the vehicle mass m, cruise speed v_{cruise}, moments of inertia I around each axis, cruise altitude H, drag coefficient C_D, and wing lift coefficient C_y for fixed-wing aircraft.

B. Weather information extraction

Weather conditions are an essential consideration in the risk assessment of aircraft. The effect of wind will affect the flight trajectory or impact speed of the aircraft after failure. In practice, scholars mainly consider the impact of wind on flight risk in two ways: weather forecast or real-time wind information.

According to ref [33], the direction of the wind and the force of the wind are obtained through the weather forecast before the flight. However, during the actual flight mission, the wind situation may be different from the weather forecast. In that situation, the authors used a stochastic manner to deal with uncertainty during the evaluation of the ground location affected by the fall impact. They chose a two-dimensional parameterization of the wind and the associated assumptions of the probability distribution, normal distribution for wind magnitude and uniform distribution for wind heading angle. Another method is to have real-time information of wind conditions during the flight. In [34], wind information achieved by using airborne sensor along with estimation algorithms, therefore no statistical assumption will be taken.

In this research, we combine the above two methods with the risk analysis assistance service. In the risk assessment process, we use wind data from the weather forecast. Also, to ensure the accuracy of the weather information, it is necessary to receive sensor information from mission aircraft in the current airspace in order to make corrections to the weather information in real time. The resistance F_{wind} received by the aircraft in the wind is shown in the following equation. In order to simplify the evaluation process, it is assumed that the windward area of the aircraft in all directions of the horizontal plane is approximately equal, which is $A_{horizontal}$. Where v_{wind} represents wind speed.

$$F_{wind} = \frac{\rho v_{wind}^2 C_D A_{horizontal}}{2} \tag{1}$$

C. Mission area information extraction

Once the flight performance parameters and weather parameters of the mission aircraft have been obtained, the environmental information of the mission area is also required for the risk assessment. This includes information on the ground traffic, population distribution, and human density, as well as information on the function of the area.

1) Traffic information: The risk value of the aircraft to the road traffic is not only related to the impact kinetic energy of the aircraft itself hitting the ground, but also related to the speed, density of vehicles on the road. The research will obtain information about the location of the road, the type of road, and the number of vehicles on the road from the overpass-turbo. The traffic density information related to time is obtained through the traffic layer of Google Maps. For risk assessment, we will combine historical traffic information as well as dynamic traffic data for road risk assessment.

2) Population information: Human population distribution behaves as a function of space and time [35]. As described in [36] and [37], government population data is aggregated for the protection of privacy. To obtain more accurate population distribution data, dasymetric mapping is proposed [38], [39]. This method uses auxiliary data to improve the resolution of population density distribution. Based on this method, the multi-class dasymmetric mapping method is developed. The area is partitioned into several residential classes (e.g., low density, medium density, high density) associated with different population densities [40]. According to [35], in cities, the diurnal population distribution varies depending on the function of the area.

In this research, the distribution of the ground population is dynamically predicted according to different type of area and mission times. The population density data obtained will be used for UAM assessment of ground-based pedestrian risk.

3) Area function information: Inspired by multi-class dasymmetric mapping method and the regularity of population density over time in different functional areas, we propose a method to assess the distribution of population density over time by using functional areas as auxiliary data. For the division of urban areas, we refer to Multidimensional Open Data of Urban Morphology (MODUM) method.

In addition to the different functional areas of the city center, the airspace in the vicinity of the airport is a factor that cannot be ignored. According to [41], the issue of flight planning risk for urban low-altitude UAVs, and traditional civil aircraft in the airspace is important for UTM-ATM integration civil manned aircraft, cruising altitudes are typically between 6,000 and 12,600 metres. However, ordinary urban air traffic aircraft operate at much lower altitudes than this. Therefore, the most likely area of conflict between the UAM and the civil aircraft is near the airport. In this research, airports are divided into different functional zones, as shown in Fig. 3, and risk is assessed based on functional zones.

In this research, a mixture of airspace consisting of structured and unstructured mission aircraft is considered. By structured mission aircraft we mean aircraft that already have a

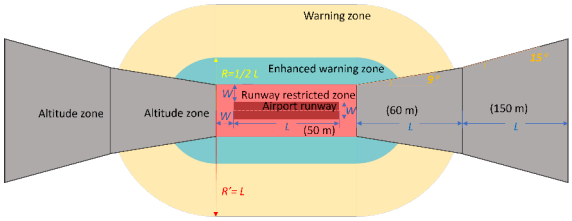

Fig. 3. Schematic diagram of the airspace division referring to the DJI GEO Zones [42].

defined flight plan, while unstructured aircraft refer to airspace intruders with uncertain flight paths or UAM experiencing emergencies. Reference to the Temporary Flight Restriction (TFR) concept proposed by the Federal Aviation Administration (FAA), in this research, multiple intruders with unknown flight routes are added to the scenarios and cylindrical TFRs are set around them.

D. Scenario-specific risk assessment

After obtaining the basic environmental information of the airspace and the information of the aircraft, a comprehensive risk assessment of the aircraft in the airspace will be conducted. According to ref [43], there might be three processes a crash incident will cause fatality: failure of UAM; the failed UAM hitting other property; and causing fatality damage after impact. Based on these three processes, the risk cost of UAM is defined as the number of fatalities per hour in this paper.

1) Risk assessment of UAM to ground and airport area: The risk cost of UAM to ground property and area near airport is calculated as Eq. (2).

$$R = P_{crash} \cdot P_{impact} \cdot P_{fatality} \tag{2}$$

Where R is the risk cost, P_{crash} is the probability of failure of the UAM, P_{impact} is the probability of impacting an object and $P_{fatality}$ is the fatality rate, which is mainly associated to the function of kinetic energy.

For the probability of an aircraft crash P_{crash}, according to [44], $1/10^5$ flight hours is used as the commercial aviation failure rate and $1/10^4$ flight hours for HPV (high-performance vehicle), $1/10^3$ flight hours for SPV (standard-performance vehicle).

The probability of impact P_{impact} is shown in Eq. (3). It is a linear function to the number of affected cars, pedestrians or aircraft. In the equation, C_{linear} is linear coefficient, $\rho_{car/people/aircraft}$ is the density of vehicles, pedestrians or aircraft in the affected area, and $A_{affected}$ is the the size of the affected area.

$$P_{impact} = C_{linear} \cdot \rho_{car/people/aircraft} \cdot A_{affected} \tag{3}$$

The fatality rate $P_{fatality}$ is related to two main factors: shelter factor $c_{shelter}$ and impact kinetic energy E_k. The shelter factor defines the shelter level when the aircraft collides with the ground property. Referring to [45], the fatality rate

$P_{fatality}$ in this paper is described by Eq. (4) where α is the impact energy that could cause 50% death with $c_{shelter}$ = 0.50, which is set to 10^6 J. β is the impact energy threshold required to cause fatality as $c_{shelter}$ approaching zero, which is set to 100 J. Ref [42], [46] elaborates on this risk assessment model and assessment process in detail.

$$P_{fatality} = \frac{1}{1 + \sqrt{\frac{\alpha}{\beta}} \left(\frac{\beta}{E_k}\right)^{\frac{1}{4c_{shelter}}}} \tag{4}$$

2) UAM mid-air collision risk assessment: In addition to considering the UAM risk to ground property and airport areas, the risk of mid-air collisions between mission UAM is also a crucial consideration.

There might be 3 processes a crash incident will cause fatality: mid-air collision of UAM; the failed UAM hitting other property; and causing fatality damage after impact. Based on these 3 processes and ref [46], the mid-air collision risk cost (R) is defined as the (5). Where P_{MAC} is the probability of UAM mid-air collision, P_{impact} is the probability to impact an object, and $P_{fatality}$ is the fatality probability, which is mainly associated to the function of kinetic energy.

$$R = P_{MAC} \cdot P_{impact} \cdot P_{fatality} \tag{5}$$

According to the SESAR ATM Barrier Model for mid-air collision [47], in the timeline of a mid-air collision, the model has different mitigation layers to prevent that a Strategic Conflict (SC) successively degenerates into a Tactical Conflict (TC), then a mid-air collision (MAC). In this research, we describe the process of mid-air collisions in terms of 3 layers of defence, which are strategic mitigation, tactical mitigation, and emergency collision avoidance. Mid-air collisions are considered to occur when the trajectory of an aerial encounter can pass right through these 3 layers.

In (5), P_{impact} and $P_{fatality}$ are calculated in a similar way to the above ground risk assessment process. For UAM mid-air collision probability P_{MAC}, this can be calculated by (6).

$$P_{MAC} = P_{SC|TC} \cdot P_{TC|CA} \cdot P_{providence} \tag{6}$$

In this equation, $P_{SC|TC}$ is the probability that after strategic mitigation, the mid-air encounter still progresses to require tactical mitigation. $P_{TC|CA}$ is the probability that after tactical conflict mitigation, the mid-air encounter still progresses to require emergency collision avoidance. The probability of a mid-air collision of the aircraft during the phase of emergency avoidance is regarded as providential $P_{providence}$. As it is rather infeasible to model "providence", we will assume a worst-case scenario where a collision must occur if the encounter between the two aircraft is no longer able to execute avoidance by the maximum overload that the aircraft can withstand, i.e. assuming that $P_{providence}$ is 1.

IV. Monte Carlo simulation

After modelling the risk of UAM operating in urban airspace, a number of different mission scenarios will be generated and the probability of having high risk conflicts in the scenarios will be counted through Monte Carlo simulations under limited conditions to assess the impact of different constraints on the capacity of the airspace.

A. Simulation scenarios definition

The mission area for the Monte Carlo simulations is defined as a rectangular airspace that includes Cranfield University, Cranfield Airport and the nearby city of Milton Keynes. The mission area is 10000 metres long and 7500 metres wide. The time chosen for the airspace capacity assessment is 6pm UK time. The mission area contains functional areas with different population densities and distributions, TFR, airport functional areas, different types of roads.

The UAM parameters that appear in the scenarios are shown in Table I. Mission UAM include HPV and SPV, and aircraft types can be classified as rotorcraft and fixed-wing aircraft. In this airspace, there are structured and unstructured aircraft. As mentioned above, structured aircraft have a defined flight plan, whereas unstructured aircraft do not have a defined flight plan and have an unpredictable future trajectory. As shown in Table I, the DJI mavic in the scenario is set up as an unstructured aircraft, which may suddenly appear anywhere in the mission airspace to simulate the threat of future unauthorised private aerial photography activity in the city. The remaining aircraft are structured aircraft and the simulation will generate their flight plans.

TABLE I
INFORMATION ABOUT THE UAM OPERATING IN SIMULATION SCENARIOS

UAM model	Type	Performance	mission
Amazon	Drone	SPV	Delivery
Cranfield eVTOL	eVTOL	HPV	Transportation
Cranfield twin mapper	Drone	SPV	Surveillance
DJI mavic pro	Drone	SPV	Photography
Ehang 216	eVTOL	HPV	Air taxi
UMILES concept 2	eVTOL	HPV	Air taxi

Before generating structured and unstructured aircraft, this research defines the UAM flight plan as unified standards for subsequent risk calculation and optimization opinions. For the purpose of this research, airspace capacity is a concept that considers time and represents the maximum number of UAM that can safely operate in a given airspace at a given time. The simulation will simulate the operation of UAM in the airspace over a period of one hour. During this hour, simulated UAM will enter the airspace at any time to perform a mission flight. The risk assessment of mid-air collisions will also take into account the current position of the UAM in the airspace at the moment.

B. Mission UAM generation

In this research, the impact of different aircraft densities, the proportion of structured and unstructured aircraft existing in same airspace, and the availability of DAA capability for structured aircraft in the airspace on the total risk-based aircraft capacity of the airspace will be investigated.

Using a Python program, a scenario containing 6 structured aircraft and 4 unstructured aircraft (intruders), not taking into account the DAA system of structured aircraft is generated, as shown in Fig. 4. Considering the randomness of generating flight plans and the manoeuvrability of the aircraft, this research will randomly select an aircraft from the above UAM participants and generate midway points randomly with reference to the maximum turning radius of that aircraft for a given start and end point, and ensure that the direct angle between the two flight plan route segments is less than the maximum turning radius.

In Fig. 4, because the structured aircraft in this mission scenario do not contain the DAA system, there may be crossover between flight plans and flight plans may cross the TFR of unstructured aircraft (intruders).

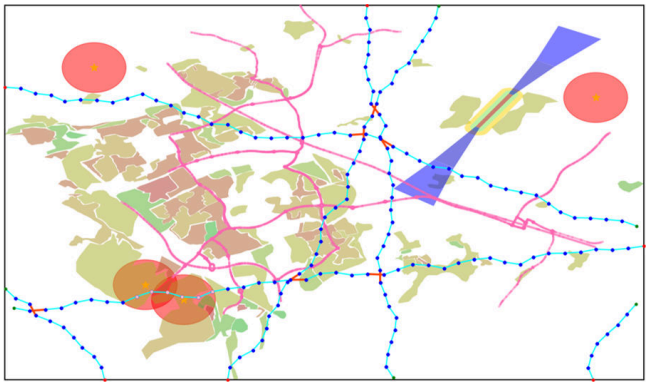

Fig. 4. Schematic of scenario with 6 structured aircraft and 4 unstructured aircraft and without DAA system. The red dots are the plan start points, the blue dots are the plan midpoints and the green dots are the plan end points. The cyan line segments are the flight route segments. The red circles are TFRs of the airspace intruders. The coloured areas show the functional areas in the city. The peach lines are the road traffic network.

All UAM in the generated scenario will be evaluated for comprehensive risk. The results of the comprehensive risk assessment for a structured aircraft are shown in Fig. 5. In the figure, the risk cost of the flight plan to ground vehicles, ground pedestrians, conventional civil aircraft and airspace intruder is assessed. The different colours of the flight plan segments in the chart represent the cost of risk for that segment. As shown in the coloured bar at the bottom of the figure, the colours range from green to red to represent the low to high risk cost.

C. Simulation error input

In order to simulate changes in the external environment and the UAM's own sensor errors during the actual mission, this research will make use of Ardupilot's Software in the Loop Simulator. The SITL (software in the loop) simulator allows users to run drone without any hardware. When running in SITL, the sensor data comes from a flight dynamics model in the flight simulator. The structure of the SITL emulator is shown in Fig. 6 (a), and a screenshot of the simulator running is shown in Fig. 6 (b).

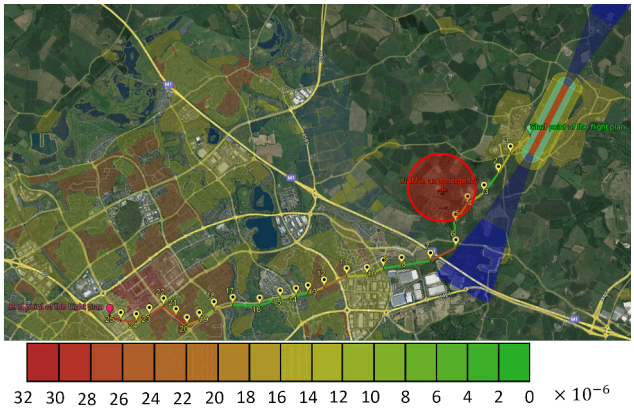

Fig. 5. Comprehensive risk assessment of the flight plan, considering the ground traffic and pedestrians, airspace near airports and intruding aircraft.

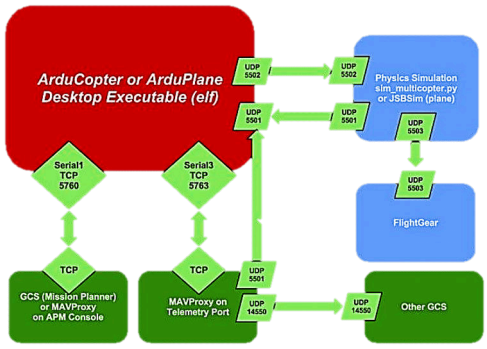

(a)

(b)

Fig. 6. Structure of the SITL simulator and its operation in the Mission Planner ground control station environment [48].

The flight errors obtained through the SITL simulator will be stored in the error database, and when using Python for Monte Carlo simulation, data from the error database will be randomly sampled to simulate the UAM errors during the mission flight. The reasons for utilising this approach rather than deploying the mission scenario simulation directly with SITL simulator are that the SITL simulation graphical interface contains a lot of unnecessary simulation information, which has a high level of computational complexity. Additionally, the SITL simulator only supports flight simulation of one aircraft.

In order to be closer to the actual mission flight situation,

sensor errors, including GPS positioning error, compass heading error, barometer altitude error, and attitude calculation error caused by vibration are incorporated. The lateral positioning error due to GPS position drift and airspeed sensor output data in the presence of external noise interference collected during a full SITL simulation mission flight are shown in Fig. 7. in Fig. 7, (a) and (b) represent the lateral positioning error and velocity sampling data during the simulation mission flight. (c) and (d) represent the pitch, roll angle, and heading angle error during simulation mission flight.

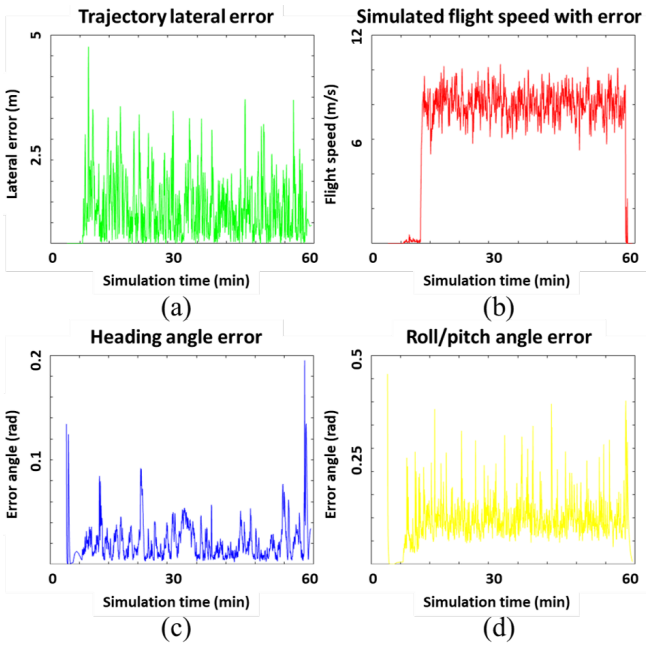

Fig. 7. Errors generated by a one-hour SITL simulated mission flight.

D. Monte-Carlo simulation setup

After completing the definition of the simulation scenarios and the different input parameters, Monte Carlo simulations are performed and the simulation results are analysed. In this research, the simulation will consider the impact of airspace aircraft density, the proportion of structured / unstructured aircraft and with / without DAA systems on airspace capacity. These different influences are combined with each other to form simulation mission scenarios. The simulation includes airspace with 5-25 aircraft, 2-4 intruders, with / without DAA systems for a total of 30 scenarios and 10,000 simulations are carried out for each mission scenario.

In order to cope with the huge amount of simulation computation, in addition to deploying the Python simulation program to different computers for collaborative computation, this research also makes use of three high-performance computing platforms, Cranfield University Delta HPC Cluster, Cranfield University DARTeC HILDA High-Performance Computing System and Amazon EC2 Elastic Compute Cloud.

The simulation process is divided into four main steps. The first step is to generate mission scenarios, which involves generating flight plans and intruders, insertion of randomly extracted errors from the SITL error library. The second step is to perform a comprehensive risk assessment of all aircraft in the scenario and extract the maximum risk value. The third step is to loop through the first two steps and store the experimental results. The fourth step is to analyse the data and generate statistical graphs based on the stored results.

E. Results analysis

The simulation results are shown in Fig. 8 and Fig. 9. Fig. 8 is the simulation result for structured aircraft in the mission scenario without on-board DAA systems, while Fig. 9 is the simulation result for structured aircraft in the mission scenario with on-board DAA systems. To ensure airspace safety, it is necessary to ensure that the maximum risk of all aircraft in the scenario is within the risk threshold, so the simulation uses the maximum risk of all participants in each scenario as the basis for evaluation. In the two figures, the horizontal coordinate represents the maximum risk value of the aircraft in the scenario, which units is defined as the number of fatalities per hour. The vertical coordinate is the frequency of occurrence of this risk value in 10,000 simulations. Subplots (a), (b), (c) represent 5, 10 and 15 structured aircraft in the airspace respectively. The red, blue, and yellow parts of the 2 figures represent 2, 3 and 4 airspace intruders respectively. By viewing the histogram of the frequency distribution of the simulation results, it can be seen that the data basically conforms to the normal distribution, showing a ”bell-shaped” distribution curve with a high middle, low sides and basic symmetry between the left and right. Therefore, the frequency distribution histograms are fitted using normal distribution curves, as shown in the curves in the 2 figures.

Finally, it is notable that in order to show the distribution of the three intruder population scenarios simultaneously, the two graphs have been panned for the frequency distribution histograms, inserting three colored frequency distribution bars in the same range, which represent three frequency distributions in the same range.

By comparing Fig. 8 and Fig. 9, it can be found that when structured aircraft contain DAA systems, the rating of mission maximum risk emergence is lower relative to scenarios without DAA systems and becomes more apparent as the density of aircraft in airspace rises. By comparing the red, blue, and yellow parts of the two figures, it can be seen that when the number of unstructured aircraft increases, the density of aircraft in the airspace will increase, and the maximum combined risk of aircraft in the airspace will also increase.

Comparing the (a), (b), (c) subplots of the two figures shows that as the total number of aircraft in the airspace increases, the maximum risk of the aircraft increases accordingly. And in terms of the distribution pattern of the maximum risk cost, when the total number of aircraft in the airspace increases, the dispersion of the risk-cost distribution of the simulation results in each case also increases. The reason for this may be that as the number of aircraft increases, the randomness of the scenario increases accordingly, requiring a greater number

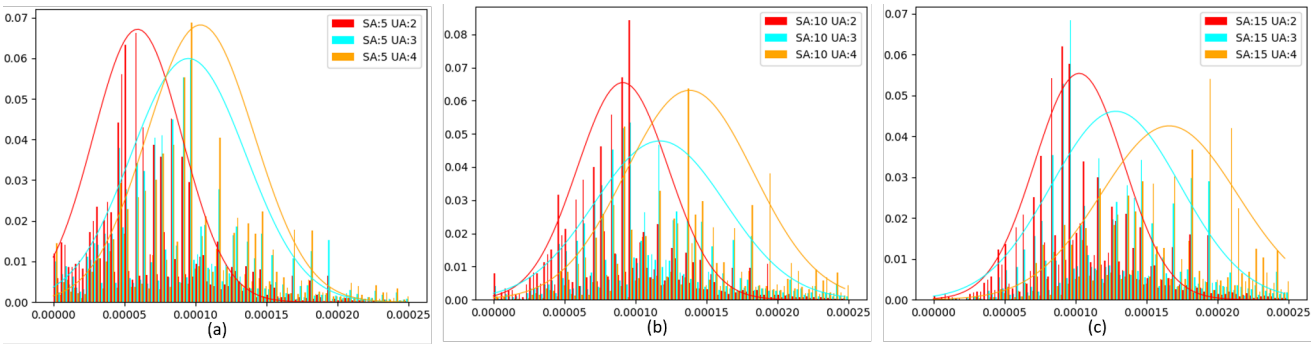

Fig. 8. Histogram of the frequency distribution of risk per 10000 simulations and fitted curve of the normal distribution for different aircraft densities and number of intruders without considering the airborne DAA system.

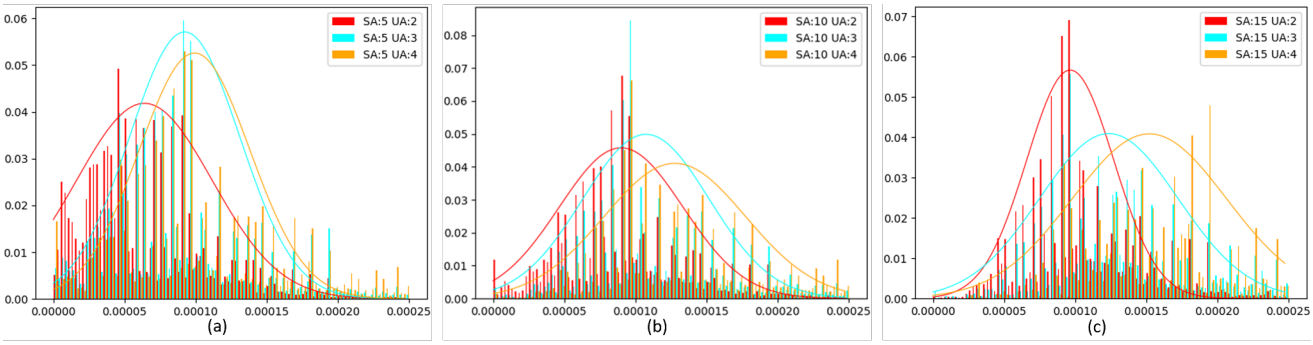

Fig. 9. Histogram of the frequency distribution of risk per 10000 simulations and fitted curve of the normal distribution for different aircraft densities and number of intruders considering the airborne DAA system.

of experiments to make the risk frequency distribution less discrete.

According to the normal distribution, 95. 449974% of the area is within two standard deviations of the mean around the mean. According to the cumulative distribution function of the normal distribution, when the risk value is equal to the mean plus twice the standard deviation, the probability that the maximum risk of the scenario is less than or equal to that risk value is 97.724987%. The mean plus twice the standard deviation of the scenario risk distribution for each mission is used as the scenario risk boundary.

Based on the risk boundary values under each scenario, the 3D risk surfaces are drawn as shown in Fig. 10 where (a) does not consider and (b) considers the aircraft on-board DAA system. With these two sub-figures it can be seen that as the number of airspace intruders and airspace aircraft increases, the combined maximum risk to the airspace will increase.

By increasing the input parameters of the scenario and increasing the number of Monte Carlo simulations, the extent of this 3D risk surface will increase and the resolution will increase. A horizontal surface is generated with the set risk threshold as the z-value to cut this 3D risk surface, and the horizontal projection of the cut interface is the airspace aircraft capacity envelope that satisfies this risk threshold condition.

Fig. 10 describes the horizontal projection of the section after cutting the 3D risk surface using different risk threshold planes. (a) does not consider and (b) considers the aircraft on-board DAA system. The different curves in the two figures represent the safe aircraft capacity envelope in the airspace at different risk thresholds. The different colours of the curves correspond to the maximum risk values shown in the rainbow bar on the right. The horizontal and vertical coordinates of the points in the area between the curves and the axes are the unstructured aircraft number and the total aircraft number that can operate safely in the airspace.

V. Conclusions and Further Research

This paper presents a risk based UAM airspace capacity assessment method using Monte Carlo simulations. The key findings are summarized below:

(1) We propose a UAM flight plan risk assessment model that quantitatively assesses the risk of UAM flight plan to air and ground and the mid-air collision risk between UAM.

(2) Using Monte Carlo simulations, we explore the impact of different airspace intruders, the total number of aircraft in the airspace, and the presence of the DAA system on the maximum comprehensive risk faced by UAM in airspace scenarios.

(3) We propose the concept of 3D risk surface and risk-based airspace capacity envelope, which will help the USSP or other service user to visually assess the maximum number of aircraft that can safely operate in the airspace at a given risk threshold.

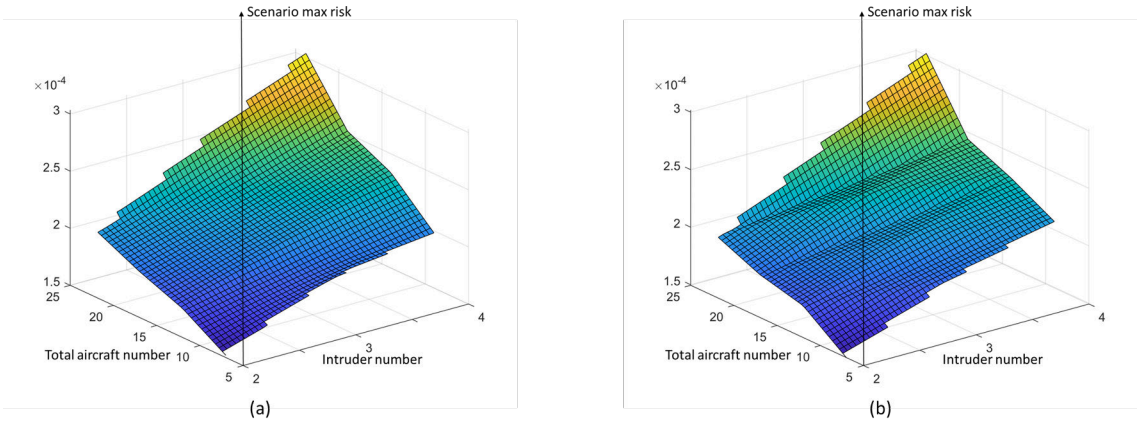

Fig. 10. 3D risk surfaces map obtained from a total of 30 scenarios with 10000 Monte Carlo simulations for each scenario with (a) / without (b) considering the airborne DAA system.

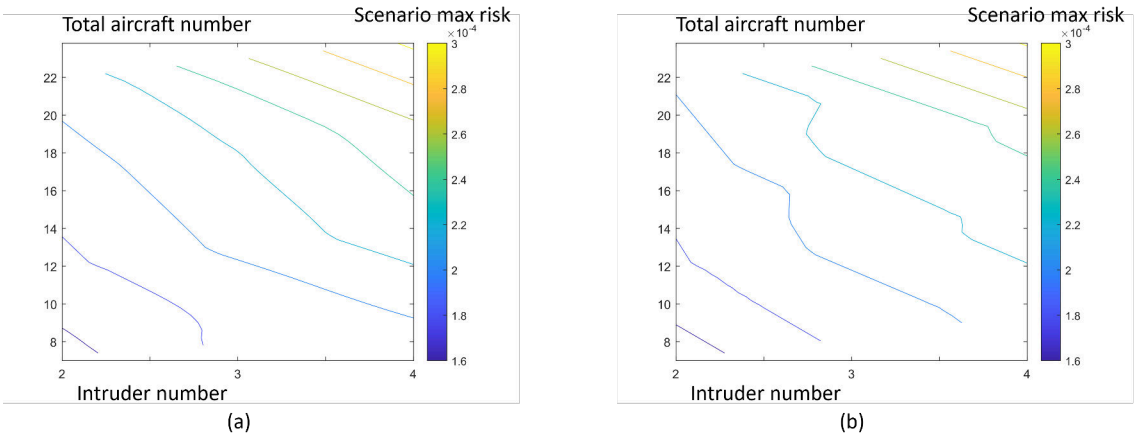

Fig. 11. Airspace capacity envelopes based on the aircraft maximum comprehensive risk threshold with (a) / without (b) considering the airborne DAA system.

For the generation of airspace simulation scenarios, only flight plans that cross the mission airspace, i.e., structured aircraft and unstructured aircraft with unknown flight plan, are considered in this research. In the future, it will be necessary to consider more airspace safety capacity considering risk thresholds under airspace structures such as Full Mix, Layers, Zones and Tubes [49]. In addition, since each scenario requires a large number of Monte Carlo simulations in order to analyze the risk distribution pattern, only up to 20 aircraft and 4 intruders in the airspace are considered in this research. Subsequent addition of more scenario simulations will increase the range and resolution of the 3D risk surface, allowing the airspace security capacity envelope to cover higher risk thresholds.

ACKNOWLEDGEMENT

This work was partially funded by the SESAR JU under grant agreement No 101017702, as part of the European Union's Horizon 2020 research and innovation programme: AMU-LED (Air Mobility Urban - Large Experimental Demonstrations). The opinions expressed herein reflect the authors view only. Under no circumstances shall the SESAR Joint Undertaking be responsible for any use that may be made of the information contained herein.

REFERENCES

[1] R Reshma, Tirumale Ramesh, and P Sathishkumar. Security situational aware intelligent road traffic monitoring using uavs. In *2016 international conference on VLSI systems, architectures, technology and applications (VLSI-SATA)*, pages 1–6. IEEE, 2016.

[2] Hamid Menouar, Ismail Guvenc, Kemal Akkaya, A Selcuk Uluagac, Abdullah Kadri, and Adem Tuncer. Uav-enabled intelligent transportation systems for the smart city: Applications and challenges. *IEEE Communications Magazine*, 55(3):22–28, 2017.

[3] Fei Qi, Xuetian Zhu, Ge Mang, Michel Kadoch, and Wei Li. Uav network and iot in the sky for future smart cities. *IEEE Network*, 33(2):96–101, 2019.

[4] Parimal Kopardekar. Urban air mobility regional readiness. Technical report, Technical report, 2019.

[5] SESAR Joint Undertaking et al. U-space: blueprint. 2017.

[6] Parimal Kopardekar, Joseph Rios, Thomas Prevot, Marcus Johnson, Jaewoo Jung, and John E Robinson. Unmanned aircraft system traffic management (utm) concept of operations. In *16th AIAA Aviation Technology, Integration, and Operations Conference*, pages 1–16. AIAA, 2016.

[7] Lorenzo Murzilli. Jarus guidelines on specific operations risk assessment (sora), 2017.

[8] Carlos Capitán, Jesús Capitán, Angel R Castano, and Aníbal Ollero. Risk assessment based on sora methodology for a uas media production application. In *2019 International Conference on Unmanned Aircraft Systems (ICUAS)*, pages 451–459. IEEE, 2019.

[9] L Murzilli et al. Jarus guidelines on specific operations risk assessment (sora), public release edition 2.0, joint authorities for rulemaking of unmanned systems, 2020.

[10] Stefano Primatesta, Giorgio Guglieri, and Alessandro Rizzo. A risk-aware path planning strategy for uavs in urban environments. *Journal of Intelligent & Robotic Systems*, 95(2):629–643, 2019.

[11] Stefano Primatesta, Alessandro Rizzo, and Anders la Cour-Harbo. Ground risk map for unmanned aircraft in urban environments. *Journal of Intelligent & Robotic Systems*, 97(3):489–509, 2020.

[12] Paul P-Y Wu, Duncan Campbell, and Torsten Merz. Multi-objective four-dimensional vehicle motion planning in large dynamic environments. *IEEE Transactions on Systems, Man, and Cybernetics, Part B (Cybernetics)*, 41(3):621–634, 2010.

[13] S Bertrand, N Raballand, F Viguier, and F Muller. Ground risk assessment for long-range inspection missions of railways by uavs. In *2017 International Conference on Unmanned Aircraft Systems (ICUAS)*, pages 1343–1351. IEEE, 2017.

[14] Sylvain Bertrand, Nicolas Raballand, and Flavien Viguier. Evaluating ground risk for road networks induced by uav operations. In *2018 International Conference on Unmanned Aircraft Systems (ICUAS)*, pages 168–176. IEEE, 2018.

[15] Andrew Hately, A Van Swalm, A Volkert, A Rushton, A Garcia, C Ronfle-Nadaud, C Barrado, D Bajiou, D Martin, DD Vecchio, et al. U-space concept of operations. In *CORUS*, 2019.

[16] Parimal Kopardekar, Jessica Rhodes, Albert Schwartz, Sherri Magyarits, and Ben Willems. Relationship of maximum manageable air traffic control complexity and sector capacity. In *26th International Congress of the Aeronautical Sciences (ICAS 2008), and AIAA-ATIO-2008-8885, Anchorage, Alaska, Sept*, pages 15–19, 2008.

[17] EG Bowen and T Pearcey. Delays in the flow of air traffic. *The Aeronautical Journal*, 52(448):251–258, 1948.

[18] Stephen LM Hockaday and Adib K Kanafani. Developments in airport capacity analysis. *Transportation Research*, 8(3):171–180, 1974.

[19] J Milan and T Vojin. Enroute sector capacity model. *Transportation Science*, 25(4):299–307, 1991.

[20] Sehchang Hah, Ben Willems, and Randy Phillips. The effect of air traffic increase on controller workload. In *Proceedings of the Human Factors and Ergonomics Society Annual Meeting*, volume 50, pages 50–54. SAGE Publications Sage CA: Los Angeles, CA, 2006.

[21] Amitabh Basu, Joseph SB Mitchell, and Girish Kumar Sabhnani. Geometric algorithms for optimal airspace design and air traffic controller workload balancing. *Journal of Experimental Algorithmics (JEA)*, 14:2–3, 2010.

[22] Ming Zhang, Ting-ting Zhang, and Songchen Han. Integrated capacity evaluation method on terminal area capacity based on the controller workload statistics. In *2010 International Conference on Optoelectronics and Image Processing*, volume 1, pages 632–636. IEEE, 2010.

[23] Jaime Rubio-Hervas, Abhishek Gupta, and Yew-Soon Ong. Data-driven risk assessment and multicriteria optimization of uav operations. *Aerospace Science and Technology*, 77:510–523, 2018.

[24] Bizhao Pang, Xinting Hu, Wei Dai, and Kin Huat Low. Third party risk modelling and assessment for safe uav path planning in metropolitan environments. *arXiv preprint arXiv:2107.01834*, 2021.

[25] Qiang Zhou and Mutian Xu. Research on risk assessment of uav to buildings. In *2021 International Conference on Information Control, Electrical Engineering and Rail Transit (ICEERT)*, pages 37–40. IEEE, 2021.

[26] Uluhan C Kaya, Atilla Dogan, and Manfred Huber. A probabilistic risk assessment framework for the path planning of safe task-aware uas operations. In *AIAA Scitech 2019 Forum*, page 2079, 2019.

[27] Christopher Lum and Blake Waggoner. A risk based paradigm and model for unmanned aerial systems in the national airspace. In *Infotech@ Aerospace 2011*, page 1424. 2011.

[28] Vishwanath Bulusu and Valentin Polishchuk. A threshold based airspace capacity estimation method for uas traffic management. In *2017 Annual IEEE International Systems Conference (SysCon)*, pages 1–7. IEEE, 2017.

[29] Vishwanath Bulusu, Valentin Polishchuk, Raja Sengupta, and Leonid Sedov. Capacity estimation for low altitude airspace. In *17th AIAA Aviation Technology, Integration, and Operations Conference*, page 4266, 2017.

[30] Jacco M Hoekstra, Ronald NHW van Gent, and Rob CJ Ruigrok. Designing for safety: the 'free flight'air traffic management concept. *Reliability Engineering & System Safety*, 75(2):215–232, 2002.

[31] James K Kuchar and Lee C Yang. A review of conflict detection and resolution modeling methods. *IEEE Transactions on intelligent transportation systems*, 1(4):179–189, 2000.

[32] Jimmy Krozel, Mark Peters, Karl D Bilimoria, Changkil Lee, and Joseph SB Mitchell. System performance characteristics of centralized and decentralized air traffic separation strategies. *Air Traffic Control Quarterly*, 9(4):311–332, 2001.

[33] Anders la Cour-Harbo. Quantifying risk of ground impact fatalities for small unmanned aircraft. *Journal of Intelligent & Robotic Systems*, 93(1):367–384, 2019.

[34] Michael Bleier, Ferdinand Settele, Markus Krauss, Alexander Knoll, and Klaus Schilling. Risk assessment of flight paths for automatic emergency parachute deployment in uavs. *IFAC-PapersOnLine*, 48(9):180–185, 2015.

[35] Budhendra Bhaduri, Edward Bright, Phillip Coleman, and Marie L Urban. Landscan usa: a high-resolution geospatial and temporal modeling approach for population distribution and dynamics. *GeoJournal*, 69(1):103–117, 2007.

[36] Serkan Ural, Ejaz Hussain, and Jie Shan. Building population mapping with aerial imagery and gis data. *International Journal of Applied Earth Observation and Geoinformation*, 13(6):841–852, 2011.

[37] Harini Sridharan and Fang Qiu. A spatially disaggregated areal interpolation model using light detection and ranging-derived building volumes. *Geographical Analysis*, 45(3):238–258, 2013.

[38] Benjamin Semenov-Tian-Shansky. Russia: Territory and population: A perspective on the 1926 census. *Geographical Review*, pages 616–640, 1928.

[39] John K Wright. A method of mapping densities of population: With cape cod as an example. *Geographical Review*, 26(1):103–110, 1936.

[40] Cory L Eicher and Cynthia A Brewer. Dasymetric mapping and areal interpolation: Implementation and evaluation. *Cartography and Geographic Information Science*, 28(2):125–138, 2001.

[41] SESAR Joint Undertaking et al. European drones outlook study: unlocking the value for europe. 2017.

[42] Yu Su, Yan Xu, and Gokhan Inalhan. A comprehensive flight plan risk assessment and optimization method considering air and ground risk of uam. In *2022 IEEE/AIAA 41st Digital Avionics Systems Conference (DASC)*, pages 1–10. IEEE, 2022.

[43] Xinting Hu, Bizhao Pang, Fuqing Dai, and Kin Huat Low. Risk assessment model for uav cost-effective path planning in urban environments. *IEEE Access*, 8:150162–150173, 2020.

[44] Enrico Petritoli, Fabio Leccese, and Lorenzo Ciani. Reliability and maintenance analysis of unmanned aerial vehicles. *Sensors*, 18(9):3171, 2018.

[45] Konstantinos Dalamagkidis, Kimon P Valavanis, and Les A Piegl. Evaluating the risk of unmanned aircraft ground impacts. In *2008 16th mediterranean conference on control and automation*, pages 709–716. IEEE, 2008.

[46] Yu Su and Yan Xu. Risk-based flight planning and management for urban air mobility. In *AIAA AVIATION 2022 Forum*, page 3619, 2022.

[47] Eurocontrol. Safety and performance requirements document for a generic surveillance system supporting air traffic control services (vol. 2), 2015.

[48] Ardupilot sitl simulator. https://ardupilot.org/dev/docs/sitl-simulator-software-in-the-loop.html.

[49] Emmanuel Sunil, Jacco Hoekstra, Joost Ellerbroek, Frank Bussink, Andrija Vidosavljevic, Daniel Delahaye, and Roalt Aalmoes. The influence of traffic structure on airspace capacity. In *7th International Conference on Research in Air Transportation*, volume 4, 2016.

A risk-based UAM airspace capacity assessment method using Monte Carlo simulation

Su, Yu

2023-11-10

Su Y, Xu Y, Inalhan G. (2023) A Risk-Based UAM Airspace Capacity Assessment Method Using Monte Carlo Simulation. In: 2023 IEEE/AIAA 42nd Digital Avionics Systems Conference (DASC), 1-5 October 2023, Barcelona, Spain

https://doi.org/10.1109/DASC58513.2023.10311149